

Vibration-insensitive fiber spool for laser stabilization

Junchao Huang (黄军超)^{1,2}, Lingke Wang (汪凌珂)^{1,2}, Yifei Duan (段怡菲)^{1,2},
Yafeng Huang (黄亚峰)^{1,2}, Meifeng Ye (叶美凤)¹, Lin Li (李琳)¹, Liang Liu (刘亮)¹,
and Tang Li (李唐)^{1,*}

¹Key Laboratory of Quantum Optics, Shanghai Institute of Optics and Fine Mechanics, Chinese Academy of Sciences, Shanghai 201800, China

²Center of Materials Science and Optoelectronics Engineering, University of Chinese Academy of Sciences, Beijing 100049, China

*Corresponding author: litang@siom.ac.cn

Received April 1, 2019; accepted May 6, 2019; posted online July 17, 2019

Excess frequency noise induced by mechanical vibration is the dominant noise source at low Fourier frequencies in fiber-delay-line stabilized lasers. To resolve this problem, a double-winding fiber spool is designed and implemented that has ultralow acceleration sensitivity in all spatial directions. By carefully choosing the optimal geometry parameters of the fiber spool, we achieve acceleration sensitivity of $8 \times 10^{-11}/g$ and $3 \times 10^{-11}/g$ (g denotes the gravitational acceleration) in axial and radial directions, respectively.

OCIS codes: 140.3425, 120.7280, 060.2310.

doi: 10.3788/COL201917.081403.

Ultrastable lasers play a vital role in the field of precision measurement science, such as optical clocks^[1–6], gravitational wave detection^[7], and very-long-baseline interferometers^[8]. State-of-the-art ultrastable lasers are realized by locking to rigid Fabry–Pérot (FP) cavities using the Pound–Drever–Hall technique. This kind of laser has achieved a fractional frequency stability below 1×10^{-16} ^[9,10]. However, the system of this powerful method is complex and bulky because it requires tight alignment of free-space optical elements, precise polarization adjustment, spatial mode matching, and even cryocooler, and consequently limits the transportable applications of ultrastable lasers. These applications include the space mission of gravitational wave detection (LISA)^[11], ultralow noise microwave synthesis^[12], and optical frequency dissemination^[13,14]. As an alternative to high-finesse FP cavities, fiber-delay-line (FDL) stabilized lasers have been demonstrated^[15–19]. Because of its all-fiber-based structure, this approach features compactness, light weight, and high reliability. The FDL stabilized laser is sensitive to seismic noise over the range from several hertz to hundreds of hertz. Environmental vibration causes fiber deformations that introduce phase fluctuations of the propagating light and convert into excess frequency noise for the stabilized laser. To overcome this problem, a fiber spool with low acceleration sensitivity is required. In the last two decades, the acceleration sensitivity of the fiber spool has been fully investigated^[20–26]. Among the above studies, Li *et al.* firstly proposed a fiber spool that could have ideal zero acceleration sensitivity along its winding axis^[21]. They wound optical fiber onto a cylinder that is vertically supported at its midplane. Under vertical vibration, the top half and the bottom half deform with the same quantity except with the opposite sign. By precisely tuning the supporting point, zero

acceleration sensitivity can be achieved. In practice, due to the large sensitivity slope, however, it is difficult to approach this “zero point” due to the unavoidable fiber-winding error and machining error. Additionally, this fiber spool cannot maintain low acceleration sensitivity in the radial (the direction in the spooling plane) and axial directions simultaneously because the “zero point” is very sensitive to the geometry parameter. To resolve this problem, Hu *et al.* proposed a fiber spool model with a symmetrically mounted structure^[22]. However, this model is not practical because of its bulky volume and complex mounting method. In this study, we propose a double-winding fiber spool with integrated support configuration. The double-winding feature can once more provide cancellation of spool deformation compared to Li *et al.*'s model, while the integrated support configuration avoids the complex mounting structure of Hu *et al.*'s model to make the fiber spool more compact and easily assembled. The numeric analysis shows that this spool can achieve acceleration sensitivities of $\sim 10^{-12}/g$ (g denotes the gravitational acceleration) in both the axial and radial directions over a range of geometry parameters.

In an FDL laser stabilization scheme, the acceleration sensitivity of the stabilized laser can be defined as^[22]

$$\Gamma_a = \frac{\Delta\nu}{\nu_0 a} = \frac{\Delta\tau}{\tau a} = \frac{\Delta L}{La}, \quad 1/g, \quad (1)$$

where ν_0 is the optical frequency, $\Delta\nu$ is the vibration-induced frequency noise, a is the vibration variation in unit of g , τ is the delay time of the FDL, $\Delta\tau$ is the vibration-induced variation of delay time, L is the fiber length, and ΔL is the vibration-induced variation of fiber length. The numeric analysis of the fiber spool is done by the finite element method (FEM) with the hypothesis that fiber

length variation follows the support surface deformation. This hypothesis is applicable when the optical fiber is precisely spooled with proper winding tension. Consequently, the acceleration sensitivity can be described in terms of the support surface deformation by the following equation:

$$\Gamma_a = \frac{\Delta S}{S a}, \quad 1/g, \quad (2)$$

where S is the initial area of the support surface, and ΔS is the variation of the surface area under the acceleration a .

Based on fiber-winding consideration, the fiber spool is usually designed as an axisymmetric configuration, while the symmetry axis is perpendicular to the spooling plane. In this work, a titanium alloy (TC4) is chosen as the material of the fiber spool because of its light weight and stiffness. By calculating the vibration-induced deformation surface area, using the FEM simulation software Patran & Nastran (MSC. Software), the acceleration sensitivity of the fiber spool is achieved.

Before introducing the new fiber spool, it is necessary to briefly analyze why Li *et al.*'s model can obtain "zero" acceleration sensitivity. Its geometry is shown in Fig. 1(a). Under vertical acceleration, the variation of the top half surface ΔS_{up} has the opposite sign to the variation of the bottom half surface ΔS_{down} . By adjusting the geometry parameter [h in this case, see Fig. 1(b)] to make $\Delta S_{\text{up}} = -\Delta S_{\text{down}}$, the zero acceleration sensitivity of the spool can be achieved. However, this deformation balance is very sensitive to both axial and radial geometry parameters. Therefore, it is difficult to maintain low axial sensitivity while optimizing the radial sensitivity by adjusting the radial parameters. Moreover, the large sensitivity slope (about $1 \times 10^{-9}/g \cdot \text{mm}$ for the parameter h) limits the possibility to obtain ultralow axial acceleration sensitivity when considering the errors in FEM simulation, spool machining, and fiber winding.

To overcome these defects, we propose a double-winding fiber spool as presented in Fig. 2. The optical fiber is wound on the top and bottom cylinder surface. Each winding cylinder is vertically supported at its midplane and has surface deformation cancellation under vertical vibration. Furthermore, the top and bottom cylinders are symmetrically supported in the vertical direction. This leads to another vertical deformation cancellation of the spool. Consequently, because of double cancellation, this spool can

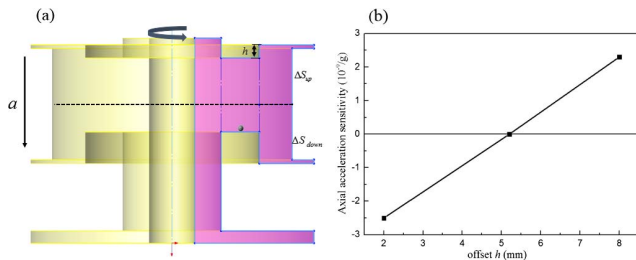


Fig. 1. (a) Geometry schematic of Li *et al.*'s model and (b) FEM calculated acceleration sensitivity versus h .

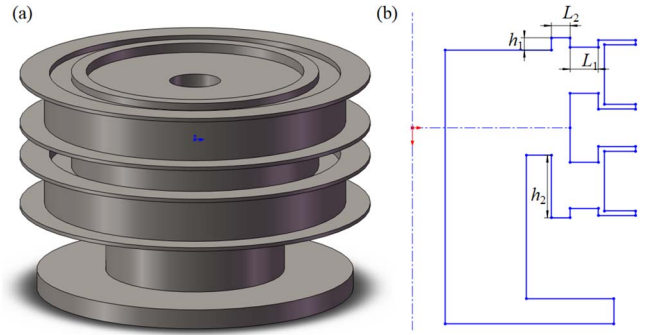


Fig. 2. (a) Double-winding fiber spool and (b) its geometry schematic.

achieve ultralow axial acceleration sensitivity that is also expected to be insensitive to the geometry parameters. We can then optimize the radial geometry parameters to achieve ultralow radial acceleration sensitivity without substantially degrading the axial sensitivity.

The optimization algorithm for the double-winding spool is depicted in Fig. 3. Initially, the sensitivity dependence on each geometric parameter was calculated. The axial sensitivity was sensitive to parameters h_1 and h_2 , while the radial sensitivity was sensitive to parameters L_1 and L_2 . After fixing other insensitive parameters, L_1 and L_2 were optimized for ultralow radial sensitivity. After fixing L_1 and L_2 , h_1 and h_2 were adjusted for optimized axial sensitivity. Finally, the radial sensitivity was re-checked. If it was not maintained, the entire procedure was repeated. The dependences of axial sensitivity on L_1 and L_2 were linear but opposite, and the slope ratio was about 1.5:1. Therefore, when the radial sensitivity was optimized, L_1 and L_2 were adjusted simultaneously at the 1.5:1 ratio to minimize the impact on the axial sensitivity. From the iteration algorithm, the optimal parameters were $h_1 = 4.4 \text{ mm}$, $h_2 = 19.5 \text{ mm}$, $L_1 = 9 \text{ mm}$, and $L_2 = 6 \text{ mm}$, with which the fiber spool had acceleration sensitivities of $-2.2 \times 10^{-12}/g$ and $-3.4 \times 10^{-12}/g$ in the axial and radial directions, respectively. Figure 4 plots the FEM calculated sensitivity for different radial and axial parameters. Both axial and radial acceleration sensitivities were insensitive to the geometric parameters and could maintain a level below $2 \times 10^{-11}/g$ over a range of parameters. In Fig. 4(b), we chose $h_2 = 19.5 \text{ mm}$ as the optimal value because the sensitivity slope at this point is close to zero and this will be helpful to avoid the influence from machining errors in the manufacture process.

The experimental setup for testing the fiber spool acceleration sensitivity is shown in Fig. 5. The measurements were performed in three steps: (1) shaking the fiber spool, (2) measuring the vibration-induced phase noise of the propagating light, and (3) measuring the transfer function of the phase noise to acceleration and calculating the acceleration sensitivity. The fiber spool was mounted on an active vibration platform that was driven by a chirp modulation signal generated with a Bode analyzer (Moku lab, Liquid Instrument). An arm-unbalanced Michelson

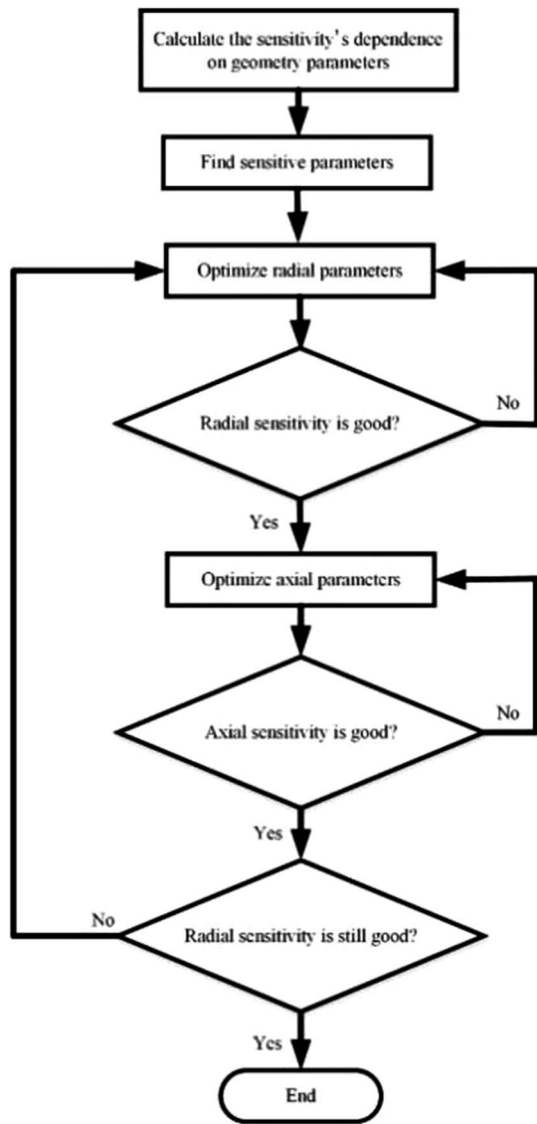


Fig. 3. Optimization algorithm for the double-winding fiber spool.

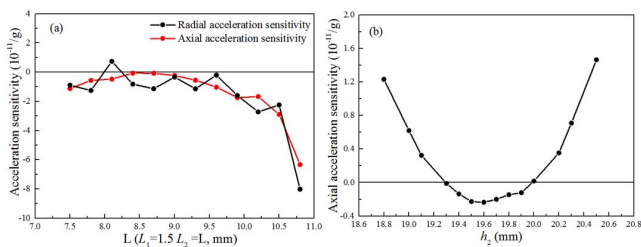


Fig. 4. FEM calculated acceleration sensitivity versus (a) L_1 and L_2 (when $h_1 = 4.4$ mm and $h_2 = 19.5$ mm) and (b) h_2 (when $L_1 = 9$ mm, $L_2 = 6$ mm, and $h_1 = 4.4$ mm).

interferometer was used to measure the vibration-induced phase noise. An acousto-optical modulator driven by 80 MHz was inserted into one arm of the interferometer after the fiber spool to shift the optical frequency for heterodyne detection, which in turn minimized noise from the laser intensity and the detection system. Moreover,

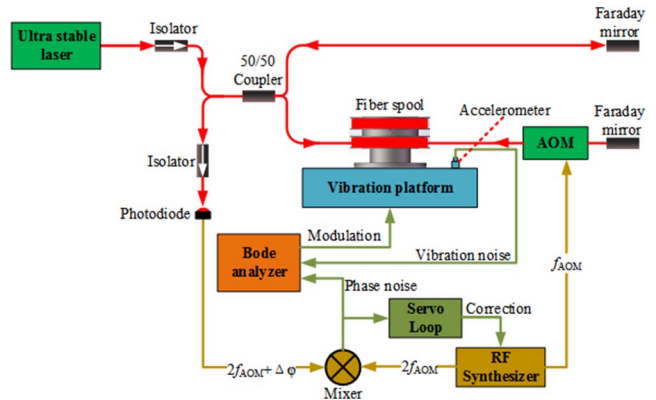


Fig. 5. Experimental apparatus for acceleration sensitivity measurements. AOM, acousto-optical modulator; RF, radio frequency.

an ultrastable laser was used to reduce residual noise from laser frequency fluctuations. At the photodiode, a radio frequency (RF) signal of 160 MHz was detected and then demodulated with the signal from an RF synthesizer to extract the phase noise. The phase noise was then split into two parts. One part was sent to a servo circuit yielding a phase-correction signal that was fed back to the RF synthesizer for maintaining phase quadrature. The time constant of the servo loop was 200 ms. Another part was sent to the Bode analyzer for the transfer function calculation with the measured vibrational noise from an accelerometer (393B04, Piezotronics Inc.). The acceleration sensitivity of the spool $\Gamma_a(f)$ was calculated by

$$\Gamma_a(f) = \frac{1}{2\pi\nu_0} \sqrt{\frac{S_\varphi(f)}{S_a(f)}} = \frac{1}{2\pi\nu_0} \Gamma_\varphi(f), \quad 1/g, \quad (3)$$

where $S_\varphi(f)$ was the vibration-induced phase noise of the propagating light, $S_a(f)$ was the measured vibration noise, and $\Gamma_\varphi(f) = \sqrt{\frac{S_\varphi(f)}{S_a(f)}}$ was the transfer function of phase noise to acceleration.

In Fig. 6, the acceleration sensitivity of the double-winding fiber spool was compared to that of the fiber spool in Ref. [21]. The two spools had the same 0.8 N winding tension and ten winding layers (the fiber length of the double-winding fiber spool is 600 m, while the fiber length of Li *et al.*'s spool is 650 m) for a standard single-mode

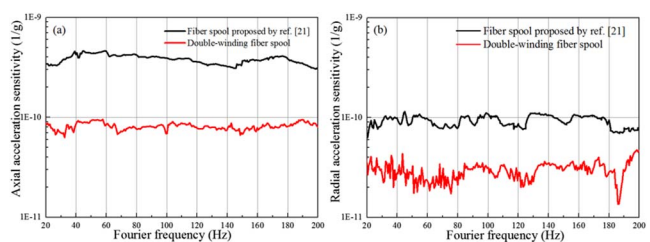


Fig. 6. Measured (a) axial and (b) radial acceleration sensitivities for different fiber spools.

fiber (SMF-28, Corning). For the double-winding fiber spool, the measured axial and radial acceleration sensitivities were $8 \times 10^{-11}/g$ and $3 \times 10^{-11}/g$, respectively. For the model of Li *et al.*, the axial sensitivity was improved by a factor of five, and the radial sensitivity was improved by a factor of three. However, the measured sensitivities were still more than an order of magnitude higher than the numerical simulations. There were three possible reasons for this discrepancy: the effect from the “free fiber” in the sensitivity measurement, the effect of winding tension, or the non-uniformity of fiber winding. In the acceleration sensitivity measurements, the fiber spool was placed on the active vibration platform, while the rest of the interferometer was placed on a vibration isolation platform and connected to the fiber spool by two 0.2 m fibers. By moving the fiber spool to the vibration isolation platform and leaving the same length of “free fiber” on the vibration platform, the residual acceleration sensitivity of the free fiber could be measured, as shown in Fig. 7. The residual acceleration sensitivity of the free fiber was $3 \times 10^{-11}/g$, which was comparable to the measured radial acceleration sensitivity of the double-winding fiber spool. Therefore, the effect of the free fiber was a major contribution in the measurement. The FEM simulation was performed under the hypothesis that the fiber length variation followed the deformation of the support surface. Therefore, the winding tension could change the extent of the deformation, and, in turn, affect the acceleration sensitivity. The acceleration sensitivity was measured for two different winding tensions (0.2 and 0.8 N), as shown in Fig. 8. For the 0.2 N winding tension, the axial and radial acceleration sensitivities both became worse because the tension was inadequate to make the fiber length change with cylinder deformation. It was possible to reduce the acceleration sensitivity by increasing the winding tension, but this also led to an increase in fiber loss and difficulty in fiber winding. In practice, a 0.8 N winding tension was acceptable. Finally, in the fiber winding process, there were inevitable gaps between two adjacent layers, especially at edges where the fiber moved to the next layer,

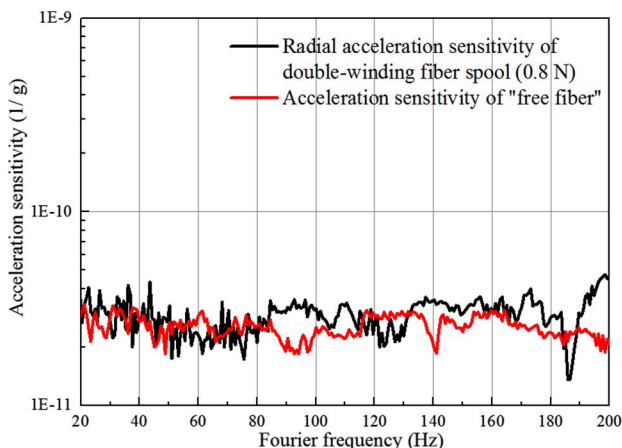


Fig. 7. Residual acceleration sensitivity of “free fiber”.

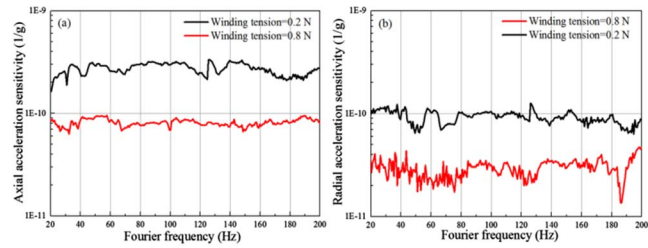


Fig. 8. (a) Axial and (b) radial acceleration sensitivities for different winding tensions.

because of fiber diameter tolerances and the winding machine. This resulted in non-uniformity between different winding layers. Consequently, the fiber moved slightly when encountering axial vibrations, degrading the axial acceleration sensitivity. It was also a reasonable explanation as to why the radial acceleration sensitivity was better than the axial sensitivity.

In conclusion, a fiber spool with ultralow acceleration sensitivities in both axial and radial directions was demonstrated for FDL laser stabilization. FEM simulations were used to numerically optimize the geometric parameters that enabled the spool to maintain an acceleration sensitivity of $\sim 10^{-12}/g$ in all spatial directions. In addition, the measured acceleration sensitivity of the fiber spool and the measured axial and radial sensitivities were $8 \times 10^{-11}/g$ and $3 \times 10^{-11}/g$, respectively, for a Fourier frequency range of 20–200 Hz. The discrepancy between the numerical analysis and the measured data was mainly derived from “free fiber”, the winding tension, and the non-uniformity of the fiber arrangement in the winding process. To improve the acceleration sensitivity of the fiber spool, the free-fiber length could be reduced, and smaller diameter optical fibers and/or hard coatings (e.g., polyimide) could be used. With this vibration-insensitive fiber spool, a compact ultrastable laser could be used without a vibration isolation platform for a variety of precision measurements. Furthermore, with the exception of laser stabilization, this fiber spool could be adopted for optoelectronic oscillators^[27].

This work was supported by the National Natural Science Foundation of China (NSFC) (Nos. 11034008, 11274324, and 11604353) and the Key Research Program of the Chinese Academy of Sciences (No. KJZD-EW-W02).

References

1. A. D. Ludlow, M. M. Boyd, J. Ye, E. Peik, and P. O. Schmidt, *Rev. Mod. Phys.* **87**, 637 (2015).
2. I. Ushijima, M. Takamoto, M. Das, T. Ohkubo, and H. Katori, *Nat. Photon.* **9**, 185 (2015).
3. N. Huntemann, C. Sanner, B. Lipphardt, C. Tamm, and E. Peik, *Phys. Rev. Lett.* **116**, 063001 (2016).
4. S. L. Campbell, R. B. Hutson, G. E. Marti, A. Goban, N. Darkwah Oppong, R. L. McNally, L. Sonderhouse, J. M. Robinson, W. Zhang, B. J. Bloom, and J. Ye, *Science* **358**, 90 (2017).

5. Y. Li, Y. G. Lin, Q. Wang, T. Yang, Z. Sun, E. J. Zang, and Z. J. Fang, *Chin. Opt. Lett.* **16**, 051402 (2018).
6. X. H. Fu, S. Fang, R. C. Zhao, Y. Zhang, J. C. Huang, J. F. Sun, Z. Xu, and Y. Z. Wang, *Chin. Opt. Lett.* **16**, 060202 (2018).
7. R. X. Adhikari, *Rev. Mod. Phys.* **86**, 121 (2014).
8. S. Doeleman, T. Mai, A. E. E. Rogers, J. G. Hartnett, M. E. Tobar, and N. Nand, *Publ. Astron. Soc. Pac.* **123**, 582 (2011).
9. S. Häfner, S. Falke, C. Grebing, S. Vogt, T. Legero, M. Merimaa, C. Lisdat, and U. Sterr, *Opt. Lett.* **40**, 2112 (2015).
10. D. G. Matei, T. Legero, S. Häfner, C. Grebing, R. Weyrich, W. Zhang, L. Sonderhouse, J. M. Robinson, J. Ye, F. Riehle, and U. Sterr, *Phys. Rev. Lett.* **118**, 263202 (2017).
11. K. Döringshoff, K. Möhle, M. Nagel, E. V. Kovalchuk, and A. Peters, in *European Frequency and Time Forum* (2010), p. 1.
12. T. M. Fortier, M. S. Kirchner, F. Quinlan, J. Taylor, J. C. Bergquist, T. Rosenband, N. Lemke, A. D. Ludlow, Y. Y. Jiang, C. W. Oates, and S. A. Diddams, *Nat. Photon.* **5**, 425 (2011).
13. O. Lopez, A. Haboucha, F. Kéfélian, H. F. Jiang, B. Chanteau, V. Roncin, C. Chardonner, A. Amy-Klein, and G. Santarelli, *Opt. Express* **18**, 16849 (2010).
14. C. Q. Ma, L. F. Wu, Y. Y. Jiang, H. F. Yu, Z. Y. Bi, and L. S. Ma, *Appl. Phys. Lett.* **107**, 261109 (2015).
15. F. Kéfélian, H. F. Jiang, P. Lemonde, and G. Santarelli, *Opt. Lett.* **34**, 914 (2009).
16. H. F. Jiang, F. Kéfélian, P. Lemonde, A. Clairon, and G. Santarelli, *Opt. Express* **18**, 3284 (2010).
17. J. Dong, Y. Q. Hu, J. C. Huang, M. F. Ye, Q. Z. Qu, T. Li, and L. Liu, *Appl. Opt.* **54**, 1152 (2015).
18. T. G. McRae, S. Ngo, D. A. Shaddock, M. T. L. Hsu, and M. B. Gray, *Opt. Lett.* **38**, 278 (2013).
19. J. C. Huang, L. K. Wang, Y. F. Duan, Y. F. Huang, M. F. Ye, L. Liu, and T. Li, *Chin. Opt. Lett.* **17**, 071407 (2019).
20. S. H. Huang, M. Tu, S. Yao, and L. Maleki, in *Proceedings of IEEE International Frequency Control Symposium and Exhibition* (2000), p. 269.
21. T. Li, B. Argence, A. Haboucha, H. F. Jiang, J. L. Dornaux, D. Kone, A. Clairon, P. Lemonde, G. Santarelli, C. Nelson, A. Hati, and E. Burt, in *Joint Conference of International Frequency Control Symposium & European Frequency and Time Forum* (2011), p. 1.
22. Y. Q. Hu, J. Dong, J. C. Huang, T. Li, and L. Liu, *Chin. Phys. B* **24**, 104213 (2015).
23. N. Ashby, D. A. Howe, J. Taylor, A. Hati, and C. W. Nelson, in *Proceedings of IEEE International Frequency Control Symposium* (2007), p. 547.
24. J. Taylor, C. W. Nelson, A. Hati, N. Ashby, and D. A. Howe, in *Proceedings of IEEE International Frequency Control Symposium* (2008), p. 807.
25. A. Hati, C. W. Nelson, J. Taylor, N. Ashby, and D. A. Howe, *IEEE Photon. Technol. Lett.* **20**, 1842 (2008).
26. C. W. Nelson, A. Hati, and D. A. Howe, *IEEE Photon. Technol. Lett.* **23**, 1633 (2011).
27. S. Yao and L. Maleki, *J. Opt. Soc. Am. B* **13**, 1725 (1996).